One step photochemical synthesis of surface-supported naked gold nanoparticles and its application as a SERS substrate

P. A. Mercadal,[a] S. D. García Schejtman,[a,b] F. P. Cometto,[a] A. V. Veglia,[b] and E. A. Coronado*[a]

A direct and straightforward method is proposed to synthetize a surface-supported gold nanoparticles mediated by pulsed laser irradiation of quartz surfaces in contact with a gold precursor solutions. The substrates´ performance as SERS sensors is tested by the Rhodamine 6G (R6G) Raman signal enhancement.

The current research on the field of nanoscience allows amazing advances in the nanofabrication techniques, giving novel nanomaterials with attractive functional properties.[1,2] In particular, noble metal nanoparticles (MNPs) have been used to develop a vast number of these nanostructures with multiple applications such as sensors, catalysts, drug delivery and photothermal therapy.[3–5] There are several methods to obtain MNPs-based nanoplatforms from top-down to bottom-up techniques including the combination of both. One of the main challenges on nanomaterials fabrication lies in developing low cost and simple processes.[6]

In the field of chemical sensing, the SERS technique is a popular and powerful tool for the ultrasensitive detection of molecules through the enhancement of the Raman signals of the molecules in close proximity to the MNP surface.[7,8] Although a number of methods have been developed for the obtention of cost-effective SERS substrates,[9–11] the fabrication of MNPs-based SERS-substrates remains a subject of current interest.[12–14]

Surface-supported MNPs can be prepared using top-down approaches such as lithography: optical, electron beam, soft, nanoimprint and polymer lithography, among others; obtaining highly ordered nanoparticle arrays.[6,15,16] However, these techniques are not quite simple to be implemented and involve several steps. Bottom-up nanofabrication approaches are another kind of useful and powerful tools for the construction of multifunctional nanostructural materials and devices by the self-assembly of atoms or molecules.[17,18] In particular, a very common bottom-up methodology widely employed to prepare SERS substrate is the chemical immobilization of NPs on quartz or glass substrates. This method requires a previously modification of solid surface, for example, with a silanization process using different organosilane compounds with functional groups that has affinity for the molecules of surface or for the MNPs.[17] Furthermore, the synthesis of MNPs are almost always related to ligands and surfactants that are bind on the surface of the NP (for example, citrate in the Turkevich's synthesis).[19] One important drawback of these methods is the possibility that the molecules used for the self-assembly process could have a SERS spectrum that give rise to a strong overlapping with the Raman modes of the analyte to be detected. In view of these shortcomings, the development of methods or techniques that surmounts the limitations of the method outlined above, is still a priority.

Hence, we introduce a fast and straightforward one-step top-down method for synthetize bare Au NPs supported on a quartz surface (AuNPs_Q) by pulsed laser irradiation of $HAuCl_4$ solution onto quartz. As a proof of concept, the performance of the AuNPs_Q platform as a sensor was evaluated using Rhodamine 6G as a SERS molecular probe. The main feature of this new method is its simplicity, fast manufacture time and that it does not require the functionalization of the solid surface, giving rise to Au NPs free of any stabilization or ligand molecule. Therefore, this platform has a great potential to be used as a SERS sensor to study a vast class of analytes, in a wide spectral range, without any interference of the Raman signals of the molecule of interest.

The experimental setup for the synthesis of the AuNPs_Q platform is sketched in Fig. 1-A. A $HAuCl_4$ 0.4 mM solution was added on a glass vessel, in order to fill it. The quartz surface was placed over the glass vessel's mouth, in contact with de $HAuCl_4$ solution. The quartz surface and the gold solution (under magnetic stirring) were vertically irradiated with a λ=532 nm pulsed laser (see SI for more details). The extinction spectra of the $HAuCl_4$ solution (without the quartz surface) before (green line) and after (blue line) several laser pulse irradiations are depicted in Fig. 1-B (3000 laser pulses, laser fluence F=510.2 mJ/cm^2, 10 Hz laser pulse frequency). It can be observed that both spectra are almost identical. The absence of an extinction mode around λ=500-600 nm after the irradiation of the $HAuCl_4$ solution indicates the non-formation of a colloidal suspension of Au NPs. The same result is also obtained if the $HAuCl_4$ solution (without the quartz surface) is irradiated using another set of laser irradiation condition (see Fig. S1). It is important to remark that the quartz surface's extinction spectrum before irradiation does not present any spectral band (see Fig. 1-B, pink line). Quite interesting, after the irradiation of the quartz surface in contact with the $HAuCl_4$ solution (by the arraignment shown in Fig. 1-A), the extinction spectrum of the quartz surface shown the characteristic localized surface plasmon (LSPR) band of Au NPs extinction intensity maximum at λ=543 (Fig. 1-B, black line). This result indicated that Au NPs were formed on the quartz face in close contact with the $HAuCl_4$ solution. The formation of AuNPs on the quartz substrate is limited to the regions where the laser beam struck on the quartz surface (it that can be appreciated as a red colour ring on the quartz surface, with the naked eye). As the area of the laser beam is

[a] *INFIQC-UNC-CONICET, Departamento de Fisicoquímica, Facultad de Ciencias Químicas, Universidad Nacional de Córdoba, Córdoba, Argentina Departamento de Físico-Química, Facultad de Ciencias Químicas, UNC.*

[b] *INFIQC-UNC-CONICET, Departamento de Química Orgánica, Facultad de Ciencias Químicas, UNC.*

†Electronic Supplementary Information (ESI) available: Extinction spectra of a 0.4 mM $HAuCl_4$ solution under different conditions of pulsed laser irradiation; Extinction spectra of the synthesized Au NPs-quartz under different conditions of pulsed laser irradiations; Extinction spectra of the AuNPs onto the quartz substrate after and before its water incubation. See DOI: 10.1039/x0xx00000x

around 0.2 cm^2, the Au NP are spread in a relatively large ring surface area.

In order to evaluate the role of the laser condition on the fabrication of these AuNPS_Q substrates, the experiments at different laser fluence and number of pulses were performed (Fig. S2). The maximum extinction intensity was obtained with 3000 laser pulses (10 Hz) and F= 510.20 mJ/cm^2. Accordingly, these are the experimental conditions chosen to perform the XPS, AFM and SERS characterization. The AuNPs_Q can be rinsed with water without any significant change of the extinction intensity (Fig. S3). These could demonstrate not only the AuNPs_Q stability but also their potential to be used several times, especially for molecules that can be easily desorbed from the Au NP surface.

The obtained bare Au NPs on a solid surface by this new and simple approach contrast with others, such as nanolithography or electrodeposition, that require large execution time and highly trained staff.[1]

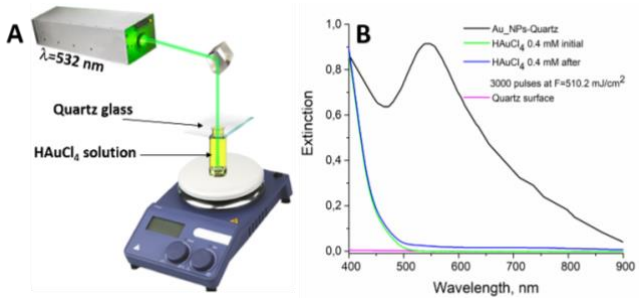

Fig. 1. A) Scheme of the experimental setup used to synthesize the AuNPs_Q. **B**) Normalized AuNPs_Q (black line) and experimental extinction spectra of a 0.4 mM $HAuCl_4$ solution, without the quartz surface, before (green line) and after (blue line) its laser irradiation. The extinction spectrum of the naked quartz substrate before the irradiation is shown in black line. In all experiments the value of laser fluence was 510.2 mJ/cm2 and 3000 laser pulses with a repetition rate of 10 Hz.

The surface chemical characterisation of the AuNPs_Q was performed by XPS measurements (Fig. 2 and Fig. S4). The elements found on the solid surface (extracted from the survey spectrum, Fig. S4) are only spurious C, Si, O, and Au. Fig. 2-A depicts two main XPS peaks located at 83.9 eV and 87.7 eV, respectively, assigned to Au4f 7/2 and Au4f 5/2. This pair of peaks is attributed to the presence of metallic gold (Au (0)) atoms forming Au NPs. Considering that the precursors on the synthesis of AuNPs_Q are Au(III) ions (and intermediate Au(I) ions), the presence of these ionic species adsorbed on the quartz surface could be expected. Nevertheless, these ionic adsorbed species should be detected at higher binding energies 85.6-89.1 eV and 87.3-90.4 eV for Au(I) and Au(III) species, respectively. The absence of these peaks indicates that the only species adsorbed on the surface are metallic Au. Regarding the Si species identified on the surface, ~90% of the signals could be assigned to SiO_2 (Si2p doublet located at 103.3 eV, typically observed on pure quartz surfaces, Fig. 2-B). Accordingly, most of the O1s peak belongs to SiO_2 (at 532.6 eV), as shown in Fig. S5. Interestingly, another Si2p doublet has been detected at lower binding energies (at 100.5 eV). This doublet could be attributed to the presence of reduced SiO_2 that serves as intermediate during AuNPs_Q synthesis.[20]

In terms of the mechanism, the experimental data suggest that $HAuCl_4$ could be reduced to Au NPs due to the generation of reactive species upon laser irradiation. The adsorbed Au NPs on the quartz surface seems to be induced by the reduction of $HAuCl_4$ in contact with the silicate surface. The XPS spectra shown that elemental Si was produced on the substrate after irradiation, this process may be due to the homolytic cleavage of Si-O bonds induced by pulsed laser irradiation and causing different reactions.

Several authors indicated similar mechanisms to form silver and gold nanoparticles that could be taking place due to the formation of oxygen and hydrogen reactive species from the decomposition of water molecules.[21–24] Moreover, Deventer and co-workers explained that the rapid adsorption/reduction of $HAuCl_4$ to Au(0) on silicate surfaces under specific conditions could be by hydrogen or silicon radicals.[20] However, these hypotheses of the synthetic mechanism were not fully verified in the present work and should be the subject of further work.

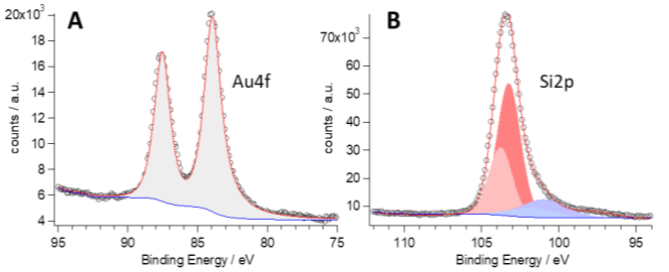

Fig. 2. XPS spectra of the **A)** Au4f and **B)** Si2p core levels showing the presence of metallic Au on the surface and two different Si contributions.

The AFM measurements also characterized the AuNPs_Q substrate (Fig. 3). The representative AFM image of the AuNPs_Q substrate (Fig. 3-A) was confirmed the presence of Au NPs on the quartz surface. Fig. 3-B shows the height profiles of Au NPs obtained from the regions highlighted with different colours in Fig. 3-A. The statistical analysis of the height profiles of the Au NPs give an average height of 27 ± 10 nm. This height profile will be used later to determine the value of the average enhancement factor obtained in the SERS experiments (see supplementary information).

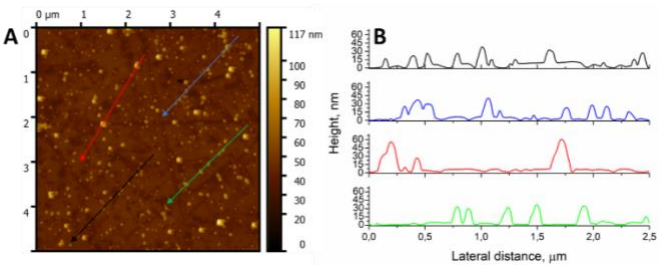

Fig. 3. A) Representative AFM image of the synthesized AuNPs_Q. B) Height profiles of the sample, the regions from which each profile was obtained are indicated in panel A as arrows with the same colour.

As was mentioned above, the AuNPs_Q substrate (without any stabilizer/linker molecules) can be potentially used as SERS

substrate in a wide spectral region. Fig. 4-A shows the Raman spectra of the quartz surface before irradiation (black line) and the obtained the AuNPs_Q (red line). 3 Raman modes was observed in both spectra, assigned to the quartz surface (between 450-800 cm^{-1}). The Raman modes at 605 and 491 cm^{-1} were attributed to oxygen-breathing associated with 3-membered and 4-membered SiO_4 rings, respectively. The Raman mode at 797 cm^{-1} could be assigned to the Si–O–Si bending/deformation mode.[25] Importantly, the Raman modes in a wide spectral range (between 800 and 3000 cm^{-1}) was not observed. This feature was quite significant since it was demonstrated the AuNPS_Q substrates should not give rise to any Raman signal overlap for most organic and inorganic molecules whose main spectral signatures are within this spectral range. As a proof of concept, the capability of AuNPs_Q to enhance the Rhodamine 6G Raman signal was tested (Fig. 4). Fig. 4-B shows the conventional Raman spectra of 1 mM R6G solution (black line), 1 μM R6G solution (blue line) and the SERS spectrum on the AuNPs_Q platform (red line). For the SERS assay, AuNPs_Q was incubated for 12 h in a 1 μM R6G solution and dried for 10 h at room temperature. The SERS spectrum shown in Fig. 4-B (red line) was the average of 15 SERS spectrum of R6G recorded in different regions of AuNPs_Q. There was an almost perfect agreement between the SERS R6G vibrational modes with the conventional Raman modes obtained in solution (black line). As the Raman modes of R6G were not observed in the 1 μM Raman spectrum (blue line), the capacity of the AuNPs_Q to enhance the Raman signal was evidenced. The variation of the intensity of the SERS signal of the AuNPs_Q substrate was determined by calculating the mean and standard deviation of the SERS intensity of the 612 and 1361 cm^{-1} Raman modes taken in 15 different regions of the SERS platform. These strong Raman modes of R6G are attributed to an in-plane bend of C-C-C ring (612 cm^{-1}) and the stretching of aromatic C-C (1361 cm^{-1}).[26,27] The average intensities are 1180 ± 245 and 1020 ± 160 counts for the 1361 cm^{-1} and 612 cm^{-1} vibrational modes, respectively (the standard deviation for both modes was shown as black error bars in the SERS spectrum of Fig. 4-B). To the SERS substrate enhancement factor (*SSEF*) for the 612 and 1361 cm^{-1} Raman modes was calculated according to the following expression:

$$SSEF = (I_{SR}/N_{SR})/(I_{RM}/N_{RM}) \qquad \text{eq. 1}$$

where I_{SR} and I_{RM} are respectively the SERS and conventional Raman intensities while N_{SR} and N_{RM} represent the number of R6G molecules in the laser scattering volume for the SERS and conventional Raman experiments, respectively.[28] The *SSEF* calculations and the experimental conditions to record the respective SERS and Raman spectra were described in the Supplementary Information. The experimental average *SSEF* values for the 1361 cm^{-1} and 612 cm^{-1} vibrational modes calculated according to eq. 1 were 2960 and 3315, respectively. The enhancement factor reported in previous work for 20-40 nm Au NPs in suspension or immobilized on a silicon substrate was 400-2000.[29,30] The *SSEF* values obtained in the present work was slightly higher, that could be attributed to the presence of Au NPs of larger size or to a weak plasmonic coupling between AuNPs and generating a slighter stronger electromagnetic field in the interparticle regions. This plasmon coupling was consistent with the LSPR spectral broadening observed in the extinction spectra in Fig. 1-B, black line. In turn, this fact agreed with the relatively large standard in the height of AuNPs_Q (27 ± 10 nm) calculated from the statistical analysis of the AFM image. However, the study of the variables that contribute to the SERS enhancement of the AuNPs_Q was beyond of this work´s scope.

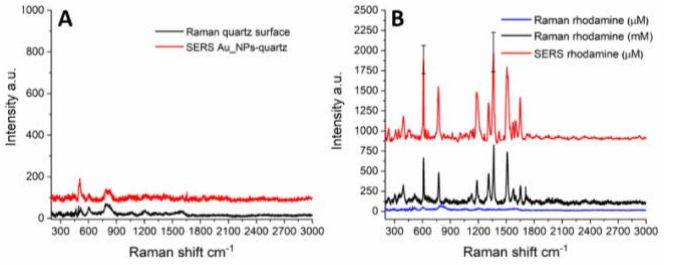

Fig 4. A) Raman spectrum of the bare quartz surface (black line) and SERS spectrum of the quartz surface in presence of the AuNPs_Q synthesized via laser irradiation (red line). B) Raman spectrum of a 1 mM (black line) and 1 μM (blue line) R6G solutions and SERS spectrum of R6G adsorbed on the AuNPs_Q substrate (red line). The black error bar represents the standard deviation of the 1361 cm^{-1} and 612 cm^{-1} Raman modes.

In summary, bare Au NPs supported on quartz surface by high-intensity pulsed laser irradiation were synthesized. The absence of stabilizing agents on the Au NPs or additional molecules that functionalize the quartz surface allows their application as a SERS sensor in a wide spectral region. As a proof of concept, SERS experiments using R6G were performed, obtaining *SSEF* values in the order of 10^3. Although this *SSEF* value was not one of the largest reported in comparison with other SERS substrates, this new approach's highlighted feature was their simplicity and quick fabrication. Finally, for a future perspective on the SERS substrate design, the fabrication of a core-shell Au@Ag NPs supported on quartz surface could be an alternative to achieve a better SERS enhancement factor value.

Conflicts of interest

There are no conflicts to declare.

Acknowledgments

The authors gratefully acknowledge financial assistance from CONICET PIP 2019-2021 (11220170100505CO). The authors also thank Agustin Tonatiuh Green Canelo (FCQ-UNC, Argentina) for his support in laser determinations. Pablo Mercadal thanks CONICET for his fellowship awarded. Dr. García Schejtman thanks PUE-CONICET for his fellowship awarded.

References

1 X. Xie, H. Pu and D.-W. Sun, *Crit. Rev. Food Sci. Nutr.*, 2018, **58**,

2800–2813.
2 B. P. Isaacoff and K. A. Brown, *Nano Lett.*, 2017, **17**, 6508–6510.
3 Z. Huang, A. Zhang, Q. Zhang and D. Cui, *J. Mater. Chem. B*, 2019, **7**, 3755–3774.
4 X. Huang and M. A. El-Sayed, *J. Adv. Res.*, 2010, **1**, 13–28.
5 F. V. Guzman, P. A. Mercadal, E. A. Coronado and E. R. Encina, *J. Phys. Chem. C*, 2019, **123**, 29891–29899.
6 A. Biswas, I. S. Bayer, A. S. Biris, T. Wang, E. Dervishi and F. Faupel, *Adv. Colloid Interface Sci.*, 2012, **170**, 2–27.
7 K. L. Kelly, E. Coronado, L. L. Zhao and G. C. Schatz, *J. Phys. Chem. B*, 2003, **107**, 668–677.
8 S. Pang, T. Yang and L. He, *TrAC - Trends Anal. Chem.*, 2016, **85**, 73–82.
9 L. Ouyang, W. Ren, L. Zhu and J. Irudayaraj, *Rev. Anal. Chem.*, **36**, 20160027.
10 T. Yaseen, H. Pu and D. W. Sun, *Trends Food Sci. Technol.*, 2018, **72**, 162–174.
11 P. A. Mosier-Boss, *Nanomaterials*, 2017, **7**, 142.
12 X. Niu, X. Li, Z. Lyu, J. Pan, S. Ding, X. Ruan, W. Zhu, D. Du and Y. Lin, *Chem. Commun.*, 2020, **56**, 11338–11353.
13 Y. Luo, Y. Xiao, D. Onidas, L. Iannazzo, M. Ethève-Quelquejeu, A. Lamouri, N. Félidj, S. Mahouche-Chergui, T. Brulé, N. Gagey-Eilstein, F. Gazeau and C. Mangeney, *Chem. Commun.*, 2020, **56**, 6822–6825.
14 X. Li, X. Duan, L. Li, S. Ye and B. Tang, *Chem. Commun.*, 2020, **56**, 9320–9323.
15 K. A. Willets and R. P. Van Duyne, *Annu. Rev. Phys. Chem.*, 2007, **58**, 267–297.
16 T. R. Jensen, M. D. Malinsky, C. L. Haynes and R. P. Van Duyne, *J. Phys. Chem. B*, 2000, **104**, 10549–10556.
17 F. Pena-Pereira, R. M. B. O. Duarte and A. C. Duarte, *TrAC - Trends Anal. Chem.*, 2012, **40**, 90–105.
18 B. Sharma, M. Fernanda Cardinal, S. L. Kleinman, N. G. Greeneltch, R. R. Frontiera, M. G. Blaber, G. C. Schatz and R. P. Van Duyne, *MRS Bull.*, 2013, **38**, 615–624.
19 J. Kimling, M. Maier, B. Okenve, V. Kotaidis, H. Ballot and A. Plech, *J. Phys. Chem. B*, 2006, **110**, 15700–15707.
20 S. Mohammadnejad, J. L. Provis and J. S. J. van Deventer, *J. Colloid Interface Sci.*, 2013, **389**, 252–259.
21 J. P. Abid, A. W. Wark, P. F. Brevet and H. H. Girault, *Chem. Commun.*, 2002, **7**, 792–793.
22 Y. H. Chen and C. S. Yeh, *Chem. Commun.*, 2001, 371–372.
23 T. Nakamura, Y. Mochidzuki and S. Sato, *J. Mater. Res.*, 2008, **23**, 968–974.
24 T. Nakamura, H. Magara, Y. Herbani and S. Sato, *Appl. Phys. A Mater. Sci. Process.*, 2011, **104**, 1021–1024.
25 G. S. Henderson, D. R. Neuville, B. Cochain and L. Cormier, *J. Non. Cryst. Solids*, 2009, **355**, 468–474.
26 P. Hildebrandt and M. Stockhurger, *J. Phys. Chem.*, 1984, **88**, 5935–5944.
27 H. Watanabe, N. Hayazawa, Y. Inouye and S. Kawata, *J. Phys. Chem. B*, 2005, **109**, 5012–5020.
28 Eric C. Le Ru and P. G. Etchegoin, *Principles of surface-enhanced Raman spectroscopy and related plasmonic effects*, Elsevier B.V., Oxford, First edit., 2009.
29 V. Joseph, A. Matschulat, J. Polte, S. Rolf, F. Emmerling and J. Kneipp, *J. Raman Spectrosc.*, 2011, **42**, 1736–1742.
30 Z. Zhu, T. Zhu and Z. Liu, *Nanotechnology*, 2004, **15**, 357–364.